JACS
JOURNAL OF THE AMERICAN CHEMICAL SOCIETY
Article
pubs.acs.org/JACS

Structural Insight into Guest Binding Sites in a Porous Homochiral Metal–Organic Material

Shi-Yuan Zhang,[†,‡] Lukasz Wojtas,[‡] and Michael J. Zaworotko*[,†]

[‡]Department of Chemical & Environmental Science, Materials and Surface Science Institute, University of Limerick, Limerick, Republic of Ireland

[†]Department of Chemistry, University of South Florida, 4202 East Fowler Avenue, CHE205, Tampa, Florida 33620, United States

Supporting Information

ABSTRACT: An enantiomeric pair of chiral metal–organic materials (CMOMs) based upon mandelate (man) and 4,4′-bipyridine (bpy) ligands, $[Co_2(S\text{-man})_2(bpy)_3](NO_3)_2\cdot$guest (**1S·guest**) and $[Co_2(R\text{-man})_2(bpy)_3](NO_3)_2\cdot$guest (**1R·guest**), have been prepared. The cationic frameworks exhibit one-dimensional chiral channels with dimensions of 8.0 Å × 8.0 Å. The pore chemistry is such that chiral surfaces lined with nitrate anions and phenyl groups create multiple binding sites for guest and/or solvent molecules. The performance of **1S** and **1R** with respect to resolution of racemic mixtures of 1-phenyl-1-propanol (PP) was studied by varying time, temperature, and the use of additives. Selectivity toward PP was determined by chiral HPLC with *ee* values of up to 60%. The binding sites and host–guest interactions were investigated through single-crystal X-ray structural analyses of guest-exchanged **1S** and **1R**. Crystallographically observed structural changes (e.g., the absolute configurations of the three PP binding sites switch from *R*, *R*, and *S* to *R*, *R*, and *R*/*S*) correlate with experimentally observed *ee* values of 33% and 60% for variants of **1S** that contain PP and different solvent molecules, **1S·PPex** and **1S·PPex′**, respectively. The fact that manipulation of guest solvent molecules, which in effect serve as cofactors, can modify chiral sites and increase enantioselectivity is likely to aid in the design of more effective CMOMs and processes for chiral separations.

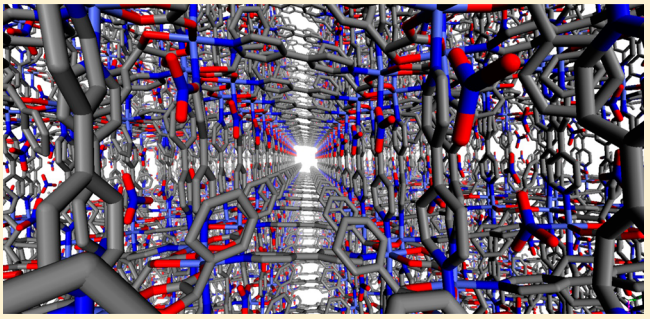

1. INTRODUCTION

The fact that metal–organic materials (MOMs)[1a] can exhibit permanent porosity has attracted considerable attention over the past 15 years.[1] An aspect of MOMs that exploits both their porosity and their fine-tunable chemical features is their ability to undergo guest exchange or to be transformed by postsynthetic modification (PSM). For example, guest exchange enables MOMs to serve as "crystal sponges" for structure eludication,[2] and chiral MOMs (CMOMs) have been studied in the context of enantioselective separation[3] and asymmetric catalysis.[4] PSM[5] can modify the pore chemistry to enhance gas sorption performance[6] or can be used to access otherwise inaccessible MOMs.[7] The most typical approach to generate CMOMs involves homochiral molecular building blocks (MBBs)[8] as opposed to relying upon spontaneous resolution of CMOMs sustained by achiral MBBs.[9] CMOMs with homochiral MBBs covalently bonded to the framework as linking or pendant ligands have been synthesized using a variety of ligands, including L-aspartate,[10] L-lactate,[11] L-alanine derivatives,[12] L-leucine derivatives,[13] L-camphorate derivatives,[14] D-tartrate derivatives,[3c] BINOL derivatives,[15] and Schiff base derivatives.[16] However, the relative cost of homochiral species and racemization during synthesis[17] have limited the development of CMOMs relative to MOMs in general.[18] Moreover, if there is a lack of control over the pore chemistry, size, and shape, then chirality in a framework does not necessarily translate into binding sites that enable strong performance in the context of enantioselective separation. The benchmark performance is exhibited by M′MOF-7, which affords *ee* values of up to 82.4% for resolution of 1-phenylethanol.[16a] However, a hydrogen-bonded network, HOF-2a, exhibits an *ee* value of 92%.[15] In most instances, much lower *ee* values are observed.[10−12,14]

Whereas the development of CMOMs in terms of network design and functionalization has been well-addressed,[13,19] the nature of the interactions that promote enantioselective separation by CMOMs has been understudied. Simply put, the combination of porosity and chirality is not on its own enough to enable strong enantioselectivity. This is partly because of the dearth of single-crystal X-ray structural studies of host–guest interactions in CMOMs, since such studies require retention of crystallinity after guest exchange and crystallographically observable guest molecules.[10,14] Indeed, there are very few structural studies that reveal the intermolecular interactions between CMOMs and chiral guests.[15,20] Herein we report the synthesis and crystal structures of a pair of novel and robust CMOMs based upon mandelate (man) and 4,4′-

Received: July 7, 2015
Published: September 7, 2015

DOI: 10.1021/jacs.5b06760
J. Am. Chem. Soc. 2015, 137, 12045−12049

bipyridine (bpy) ligands, $[Co_2(S\text{-man})_2(bpy)_3](NO_3)_2\cdot$guest (**1S·guest**) and $[Co_2(R\text{-man})_2(bpy)_3](NO_3)_2\cdot$guest (**1R·guest**). Our study reveals that relatively high *ee* values can be achieved through confined space that exploits the homochirality of the MBBs through van der Waals forces, hydrogen-bonding interactions, and $\pi-\pi$ stacking interactions. Furthermore, the role that the solvent can play as a cofactor at binding sites is delineated.

2. EXPERIMENTAL SECTION

2.1. Materials and Synthesis. All of the reagents and solvents were commercially available and used as received.

*2.1.1. Synthesis of **1S·NB** and **1R·NB**.* A 5 mL methanol solution of 0.4 mmol of $Co(NO_3)_2\cdot 6H_2O$ (120 mg) and 0.4 mmol of enantiopure mandelic acid (*S* isomer for **1S** and *R* isomer for **1R**, 60.8 mg) was layered above a 5 mL nitrobenzene (NB) solution of 0.3 mmol of bpy (46.8 mg). A 5 mL 1:1 methanol/nitrobenzene buffer solution was layered between the top and bottom layers to allow slow diffusion for 7 days. Red rectangular prismatic crystals were obtained in ∼50% yield.

*2.1.2. Synthesis of Solvent-Exchanged Variants **1S·guest** and **1R·guest**.* Crystals of as-synthesized **1S·NB** and **1R·NB** were exchanged with DCM daily for 5 days, affording **1S·DCM** and **1R·DCM**. Desolvated **1S** and **1R** were obtained from **1S·DCM** and **1R·DCM**, respectively, under vacuum. **1S·CH** and **1R·CH** were prepared by immersing crystals of **1S** and **1R**, respectively, in cyclohexane (CH) for 7 days. Single crystals of **1S·PPex** were prepared by soaking **1S·DCM** in racemic PP for 7 days. Another variant, **1S·PPex′**, was prepared by soaking desolvated **1S** in racemic PP in the presence of 200 μL of 90% $MeOH/H_2O$ for 5 days.

2.2. Characterization. *2.2.1. Physical Measurements.* Powder X-ray diffraction (PXRD) was performed on a Bruker D8 Venture diffractometer using Cu Kα radiation (λ = 1.5418 Å). Thermogravimetric analysis (TGA) was performed using a TA Instruments TGA-Q50 analyzer at a constant heating rate of 5 °C/min from 25 to 800 °C. UV−vis spectra were measured using a JASCO J-715 spectrometer. FT-IR spectra were recorded on a PerkinElmer Spectrum Two spectrometer. HPLC measurements were carried out on a Shimadzu HPLC system with a Chiralcel OD-H column using a flow rate of 1 mL/min.

2.2.2. Crystallographic Studies. Crystals of as-synthesized **1S·NB** and **1R·NB** and guest-exchanged **1S·CH**, **1S·PPex**, and **1S·PPex′** were chosen for single-crystal X-ray diffraction studies. The data were collected on a Bruker D8 Venture PHOTON 100 CMOS system equipped with a Cu Kα INCOATEC Imus microfocus source (λ = 1.54178 Å, T = 100(2) K). In all cases, indexing was performed using APEX2.[21] Data integration and reduction were performed using SaintPlus 6.01.[22] Absorption corrections were performed by the multiscan method as implemented in SADABS.[23] Space groups were determined using XPREP as implemented in APEX2. Structures were solved using the Patterson method (SHELXS-97), expanded using Fourier methods, and refined on F^2 using nonlinear least-squares techniques with SHELXL-97 contained in APEX2 and WinGX version 1.70.01.[24−27] Crystallographic data for the as-synthesized and guest-exchanged CMOMs are summarized in Tables S1 and S2, respectively. Refinement details concerning the PP guest molecules are given in the Supporting Information.

2.3. Chiral Resolution of PP. The crystals used to study chiral resolution were obtained from layering and used as synthesized. **1S·DCM** and **1R·DCM** were immersed in 1 mL of racemic PP with no stirring or shaking for various time periods and temperatures, as detailed in Tables 1 and S3. The desolvated materials **1S** and **1R** were treated using a similar procedure except that varying amounts of $MeOH/H_2O$ solutions were used as additives (Tables 2 and S4). After specific time periods, crystals were filtered and washed with CH (6 × 1 mL) to remove the residual PP from the surface of the crystals. DCM was then used to successively extract PP from the crystals (8 × 0.5 mL). The resulting extracts were monitored by TLC to ensure that all of the encapsulated PP had indeed been released. The filtrates were combined and analyzed by chiral HPLC to determine *ee* values, and UV−vis spectroscopy was used to determine the loading. The resulting crystals were dried in air and weighed (the weights ranged from 0.03 to 0.04 g). A standard calibration curve for PP was generated (Scheme S1), and the loading of PP was calculated as $(n_{PP,exptl}/n_{PP,calcd}) \times 100\%$, where $n_{PP,exptl}$ and $n_{PP,calcd}$ are the experimental and calculated numbers of moles of PP, respectively. The chiral resolution procedure is expressed in the form of a flowchart in Scheme S2. HPLC data for the resolution of PP are presented in Figures S9−S53.

3. RESULTS AND DISCUSSION

1S·NB and **1R·NB** were prepared by slow diffusion of a solution of $Co(NO_3)_2\cdot 6H_2O$ and (*S*)- or (*R*)-mandelic acid, respectively, in MeOH into 1:1 methanol/nitrobenzene that had been layered over a nitrobenzene solution of bpy. Single-crystal X-ray diffraction analysis of **1S·NB** and **1R·NB** revealed that they are isostructural, crystallizing in the chiral space group $P2_1$. The structure of **1S·NB** is sustained by Co^{2+} ions linked by (*S*)-mandelate anions so as to form one-dimensional (1D) chiral chains running parallel to the *a* axis (Figure 1a). These

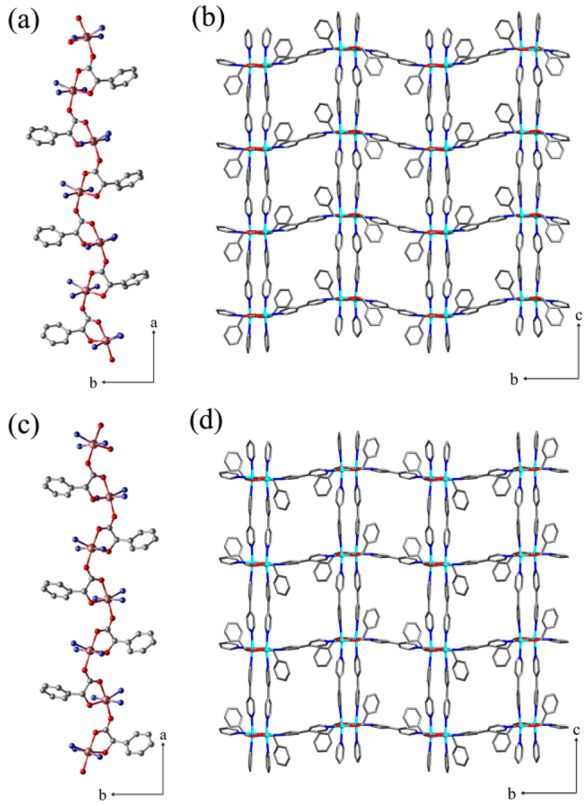

Figure 1. (left) 1D chiral chains linked by (a) (*S*)-mandelate in **1S** and (c) (*R*)-mandelate in **1R**. (right) Projections of the structures of (b) **1S** and (d) **1R** from above the *bc* plane. Hydrogen atoms, nitrate anions, and solvent molecules have been omitted for the sake of clarity.

chains are cross-linked by bpy linkers in the other two directions to form a three-dimensional network with the **bnn** topology (Figure 1b). The structure of **1R·NB** is of the opposite chirality (Figure 1c,d). The pore size of the 1D channels in **1S·NB** and **1R·NB** is defined by the length of the bpy linkers (Figure S1) and is ca. 8.0 Å × 8.0 Å after subtraction of the van der Waals radii. The pore chemistry and shape are controlled by the chiral mandelate linkers and nitrate counterions, resulting in uneven pore surfaces. The void volume of the pores was calculated using PLATON[21] to be 33% of the unit cell volume. The pores of the as-synthesized

DOI: 10.1021/jacs.5b06760
J. Am. Chem. Soc. 2015, 137, 12045−12049

crystals of **1S·NB** and **1R·NB** are occupied by nitrobenzene. The positions and binding sites of NB inside the channels are shown and described in Figure S2.

We examined the ability of **1S·DCM** and **1R·DCM** to resolve racemic PP following procedures detailed in the Experimental Section. We selected PP for study because it is an important intermediate in the synthesis of pharmaceutical and parasiticide compounds.[3,28] PP-exchanged **1S** materials were characterized by PXRD (Figure S4) and FT-IR spectroscopy (Figure S5). Table 1 reveals that **1S·DCM** and **1R·DCM** that had been soaked in racemic PP for 7 days exhibited higher *ee* values (32% and 30%, respectively) than samples exposed to PP for shorter time periods. The loading amount of PP was also observed to increase gradually from 82% to 96% within 5 days. However, a further 2 days of exposure resulted in a decreased loading of PP. We attribute this effect to partial loss of crystallinity of the bulk sample, as suggested by broadening of the PXRD peaks (Figure S4). PP/additive-exposed crystals also appeared to start losing crystallinity within 5 days. Conversely, PXRD profiles of **1S** soaked in CH were unchanged after 1 month (Figure S3). TGA indicated that **1S** is stable to 200 °C (Figure S6). When resolution of PP was conducted at 40 °C, the *ee* values remained at ∼26% from 1 day to 5 days (Table S3). However, the loading of PP started to decrease after only 3 days. These results indicate that 5 days at room temperature are optimal conditions for conducting separations since slow amorphization thereafter reduces the loading.

Table 1. Resolution of PP by 1S·DCM and 1R·DCM at Room Temperature over Different Time Periods

CMOM	time (days)	(*S*)-PP:(*R*)-PP[a]	*ee* [%][a]	loading [%][b]
1S·DCM	1	41:59	18	82
	3	39:61	22	88
	5	39:61	22	96
	7	34:66	32	70
1R·DCM	1	58:42	16	83
	3	61:39	22	88
	5	62:38	24	97
	7	65:35	30	71

[a]Determined by HPLC analysis using a chiral OD stationary phase. [b]The total amount of released PP was determined by UV−vis spectroscopy using a PP calibration curve.

To test the effect of additives on the performance, resolution experiments using **1S·DCM** and **1R·DCM** desolvated by vacuum were conducted. **1S** and **1R** were soaked in racemic PP in the presence of varying amounts of MeOH/H_2O under the optimal conditions found for pure PP, i.e., room temperature for 5 days. As detailed in Table 2, in the absence of MeOH/H_2O, *ee* values of 34% with loadings of 96% and 95%, respectively, were observed. As the amount of MeOH/H_2O was increased from 10 to 50 μL, the *ee* values remained largely unchanged (∼30% for **1S** and 38% for **1R**). However, the loading of PP decreased from 99% (98%) to ∼82% (86%) for **1S** (**1R**), indicating competition for the PP guest binding sites from MeOH/H_2O, accelerated amorphization, or both. The highest *ee* value (60%) was observed with 200 μL of 90% MeOH/H_2O, but the loading was only 33%. Nevertheless, to our knowledge this performance is 1.7 times higher than that reported for any other porous MOM.[12] Further experiments were conducted at 40 °C for 1 day (Table S4), and the *ee* values were observed to improve gradually as the MeOH/H_2O ratio was increased. However, once again the loading of PP dropped, this time from 98% to 28%.

Table 2. Resolution of PP by 1S and 1R at Room Temperature for 5 days

CMOM[a]	additive [μL, %][b]	(*S*)-PP:(*R*)-PP[c]	*ee* [%][c]	loading [%][d]
1S	0, 0	33:67	34	96
	10, 50	30:70	40	99
	10, 90	35:65	30	97
	50, 50	35:65	30	83
	50, 90	34:66	32	82
	100, 90	25:75	50	72
	200, 90	20:80	60	33
1R	0, 0	67:33	34	95
	10, 50	69:31	38	98
	10, 90	69:31	38	97
	50, 50	69:31	38	86
	50, 90	69:31	38	86
	100, 90	72:28	46	70
	200, 90	76:24	52	30

[a]The desolvated materials were obtained from **1S·DCM** and **1R·DCM** under vacuum. [b]Total volume (left) of an *x*% v/v (right) MeOH aqueous solution used as an additive in 1 mL of racemic PP. [c]Determined by HPLC analysis using a chiral OD stationary phase. [d]The total amount of released PP was determined by UV−vis spectroscopy using a PP calibration curve.

The fact that **1S** and **1R** retained their crystallinity after solvent/guest exchange for at least several days enabled us to use single-crystal X-ray crystallography to study the nature of the interactions between various guest molecules and the pore surfaces of **1S** and **1R**. For example, soaking crystals of **1S** in cyclohexane afforded **1S·CH**, in which CH molecules lie in ordered positions and interact with phenyl groups and nitrate ions (Figure S7).

In order to better understand the enantioselectivity of **1S** toward racemic PP, we also determined the single-crystal structures of **1S·PPex** and **1S·PPex′**. The unit cells of **1S·PPex** and **1S·PPex′** are double those of **1S·NB** and **1S·CH**. Figures 2 and 3 provide insight as to why there is doubling of the unit cell

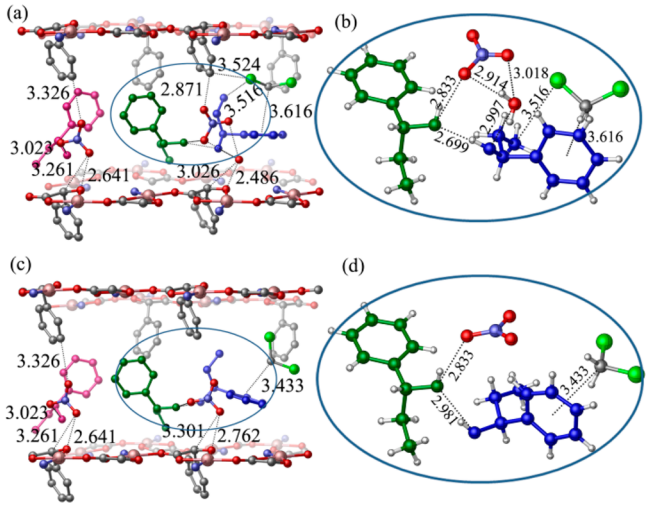

Figure 2. Locations of the three crystallographically independent PP molecules (colored magenta, green, and blue) in **1S·PPex**. The third PP molecule is disordered over two positions, one shown in (a) and (b) and the other in (c) and (d).

DOI: 10.1021/jacs.5b06760
J. Am. Chem. Soc. 2015, 137, 12045−12049

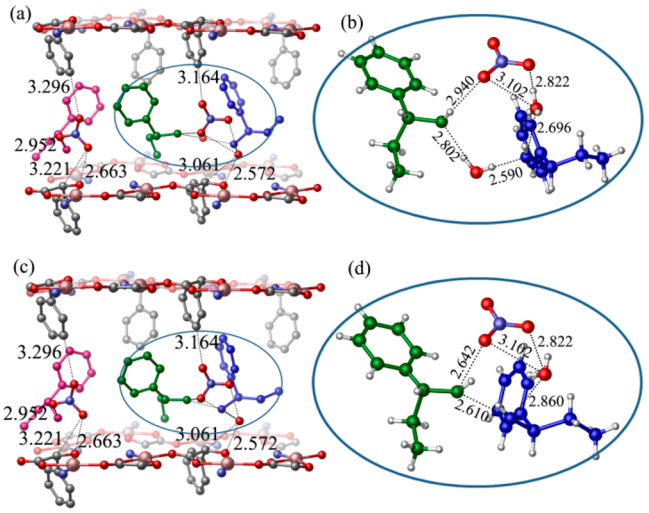

Figure 3. Locations of the three crystallographically independent PP molecules (colored magenta, green, and blue) in **1S·PPex′**. The second and third PP molecules are disordered over two positions, one shown in (a) and (b) and the other in (c) and (d).

and why **1S·PPex** binds (*R*)-PP in preference to (*S*)-PP in **1S·PPex′**. There are three distinct PP binding sites. The first and second binding sites are similar. Specifically, hydroxyl groups from PP molecules form O−H···O hydrogen bonds with nitrate anions with contact distances of 3.023/2.833 Å and 2.934/2.892 (2.665) Å in **1S·PPex** and **1S·PPex′**, respectively. The most notable difference between the two structures is the direction, position, and conformation of the third PP molecule. The third PP molecule is disordered over two positions, as illustrated in Figures 2 and 3. In **1S·PPex**, a DCM molecule participates in a hydrogen-bonded ring (Figure 2b) involving the nitrate anion, the second PP, and the third PP. Additional close contacts between DCM and PP molecules with Cl···H−C_{ethyl} and C−H···π_{phenyl} distances of 3.516 and 3.616 Å, respectively, occur. In the other disordered position (Figure 2d), the third PP interacts with the hydroxyl group of the second PP (O−H···O, 2.981 Å) and DCM (π···H−C, 3.433 Å), causing it to be oriented nearly parallel with respect to the *bc* plane. The third PP molecule is resolved as the *R* enantiomer, meaning that the maximum *ee* value according to the crystal structure is 33% (a selectivity of 2:1 for (*R*)-PP over (*S*)-PP). In contrast, disordered water/methanol molecules in **1S·PPex′** participate in a cyclic hydrogen-bonded ring (Figure 3b) involving a nitrate anion with the second and third PP molecules. This arrangement forces the third PP molecule to be oriented closer to perpendicular with respect to the *bc* plane. Figure 3d reveals that an intermolecular hydrogen-bonding interaction between the second and the third PP molecules (C−H···O, 2.356 Å) enables these PP molecules to lie in close proximity.

The change in orientation of the third PP could be responsible for the enantioselectivity for (*S*)-PP in **1S·PPex** relative to (*R*)-PP in **1S·PPex′**. Figure 4 illustrates that the binding sites are distinctly different even though most of the components around the binding site are unchanged. Further, the hydroxyl groups of the third PP are fixed in both structures through hydrogen bonding to a nitrate anion and a water molecule. However, the DCM and water/methanol molecules in **1S·PPex** and **1S·PPex′**, respectively, profoundly impact the shape of the binding site. Specifically, the DCM molecule

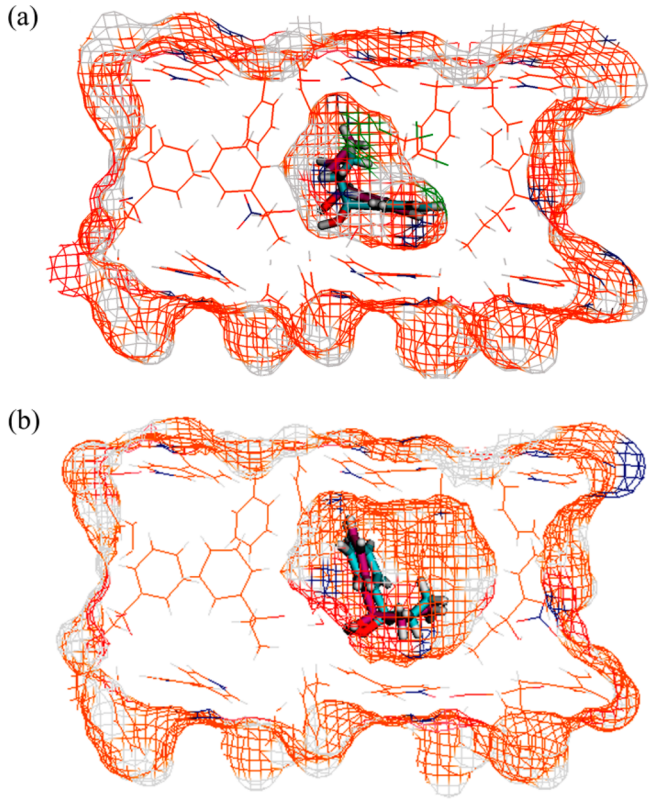

Figure 4. Perspective view of the binding sites occupied by the third PP molecule in **1S·PPex** (a) and **1S·PPex′** (b). The color of the mesh represents the element that generates the corresponding part of the surface: C, orange; O, red; N, blue; Cl, green; H, white. The first and second binding sites are illustrated in Figure S8.

compresses the width of the cavity (Figure 4a) and prevents the phenyl group from aligning perpendicular to the *bc* plane. Conversely, the water/methanol molecule reduces the length of the cavity (Figure 4b) and prevents the phenyl group from lying parallel to the *bc* plane. The overall effect of these structural changes is that there is higher enantioselectivity for the third PP in **1S·PPex′**. This effect is reminiscent of changing an enzyme's preference for cofactors.

1S·PPex′ exhibits 60% *ee* for PP according to HPLC analysis, but this is lower than expected from our crystallographic analysis. However, lower than expected *ee* values have also been observed by other groups,[10,29,30] presumably because of disorder of guest molecules in host channels. Gaining an understanding of the reasons for this lack of specificity of the chiral binding sites is necessary in order to design materials with even better *ee* performance.

4. CONCLUSION

We have reported the single-step synthesis of a pair of robust CMOMs from commercially available chemicals. Thanks to the 1D homochiral channels within **1S** and **1R**, enantioselective recognition toward PP was observed with *ee* values of up to 60%. Our study of the crystal structures of variants of **1S·PP** reveals how DCM and water/methanol molecules can play an important role in affecting the shape of the binding sites for PP. Indeed, manipulation of the guest solvent molecules, which in effect serve as cofactors, can be used to modify a PP binding site and increase the overall enantioselectivity. Further studies will be conducted to address the effect of pore size and pore

DOI: 10.1021/jacs.5b06760
J. Am. Chem. Soc. 2015, 137, 12045−12049

chemistry on the enantioselectivity toward PP and other chiral guest molecules.

■ ASSOCIATED CONTENT

Supporting Information

The Supporting Information is available free of charge on the ACS Publications website at DOI: 10.1021/jacs.5b06760.

Characterization data and supplementary schemes, tables, and figures (PDF)
Crystallographic data for **1S-NB** (CIF)
Crystallographic data for **1R-NB** (CIF)
Crystallographic data for **1S-PPex′** (CIF)
Crystallographic data for **1S-PPex** (CIF)
Crystallographic data for **1S-CH** (CIF)

■ AUTHOR INFORMATION

Corresponding Author

*xtal@ul.ie

Notes

The authors declare no competing financial interest.

■ ACKNOWLEDGMENTS

This work was supported by the U.S. Department of Energy (DE-AR0000177) and the Science Foundation of Ireland (Award 13/RP/B2549). We thank Prof. Peter Zhang's group for their assistance with collection of HPLC data.

■ REFERENCES

(1) (a) Perry, J. J., IV; Perman, J. A.; Zaworotko, M. J. *Chem. Soc. Rev.* **2009**, *38*, 1400. (b) Batten, S. R.; Neville, S. M.; Turner, D. R. *Coordination Polymers: Design, Analysis and Application*; Royal Society of Chemistry: Cambridge, U.K., 2009. (c) MacGillivray, L. R. *Metal–Organic Frameworks: Design and Application*; John Wiley & Sons: Hoboken, NJ, 2010.

(2) (a) Inokuma, Y.; Yoshioka, S.; Ariyoshi, J.; Arai, T.; Hitora, Y.; Takada, K.; Matsunaga, S.; Rissanen, K.; Fujita, M. *Nature* **2013**, *495*, 461. (b) Inokuma, Y.; Arai, T.; Fujita, M. *Nat. Chem.* **2010**, *2*, 780. (c) Fujita, D.; Suzuki, K.; Sato, S.; Yagi-Utsumi, M.; Yamaguchi, Y.; Mizuno, N.; Kumasaka, T.; Takata, M.; Noda, M.; Uchiyama, S.; Kato, K.; Fujita, M. *Nat. Commun.* **2012**, *3*, 1093.

(3) (a) Kim, K.; Banerjee, M.; Yoon, M.; Das, S. *Top. Curr. Chem.* **2009**, *293*, 115. (b) Liu, Y.; Xuan, W.; Cui, Y. *Adv. Mater.* **2010**, *22*, 4112. (c) Seo, J. S.; Whang, D.; Lee, H.; Jun, S. I.; Oh, J.; Jeon, Y. J.; Kim, K. *Nature* **2000**, *404*, 982.

(4) (a) Lee, J.; Farha, O. K.; Roberts, J.; Scheidt, K. A.; Nguyen, S. T.; Hupp, J. T. *Chem. Soc. Rev.* **2009**, *38*, 1450. (b) Yoon, M.; Srirambalaji, R.; Kim, K. *Chem. Rev.* **2012**, *112*, 1196.

(5) (a) Cohen, S. M. *Chem. Rev.* **2012**, *112*, 970. (b) Valtchev, V.; Majano, G.; Mintova, S.; Pérez-Ramírez, J. *Chem. Soc. Rev.* **2013**, *42*, 263. (c) Yoon, M.; Srirambalaji, R.; Kim, K. *Chem. Rev.* **2012**, *112*, 1196.

(6) (a) Tanabe, K. K.; Cohen, S. M. *Chem. Soc. Rev.* **2011**, *40*, 498. (b) Li, J.-R.; Ma, Y.; McCarthy, M. C.; Sculley, J.; Yu, J.; Jeong, H.-K.; Balbuena, P. B.; Zhou, H.-C. *Coord. Chem. Rev.* **2011**, *255*, 1791. (c) Mulfort, K. L.; Farha, O. K.; Stern, C. L.; Sarjeant, A. A.; Hupp, J. T. *J. Am. Chem. Soc.* **2009**, *131*, 3866.

(7) (a) Zhang, Z.; Zhang, L.; Wojtas, L.; Nugent, P.; Eddaoudi, M.; Zaworotko, M. J. *J. Am. Chem. Soc.* **2012**, *134*, 924. (b) Deria, P.; Mondloch, J. E.; Karagiaridi, O.; Bury, W.; Hupp, J. T.; Farha, O. K. *Chem. Soc. Rev.* **2014**, *43*, 5896.

(8) (a) Ma, L.; Abney, C.; Lin, W. *Chem. Soc. Rev.* **2009**, *38*, 1248. (b) Anokhina, E.; Go, Y.; Lee, Y.; Vogt, T.; Jacobson, A. *J. Am. Chem. Soc.* **2006**, *128*, 9957. (c) Morris, R.; Bu, X. *Nat. Chem.* **2010**, *2*, 353. (d) Dybtsev, D. N.; Yutkin, M. P.; Peresypkina, E. V.; Virovets, A. V.; Serre, C.; Férey, G.; Fedin, V. P. *Inorg. Chem.* **2007**, *46*, 6843.

(9) (a) Pérez-García, L.; Amabilino, D. *Chem. Soc. Rev.* **2002**, *31*, 342. (b) Biradha, K.; Seward, C.; Zaworotko, M. J. *Angew. Chem., Int. Ed.* **1999**, *38*, 492. (c) Kepert, C. J.; Prior, T. J.; Rosseinsky, M. J. *J. Am. Chem. Soc.* **2000**, *122*, 5158.

(10) Vaidhyanathan, R.; Bradshaw, D.; Rebilly, J.-N.; Barrio, J. P.; Gould, J. A.; Berry, N. G.; Rosseinsky, M. J. *Angew. Chem., Int. Ed.* **2006**, *45*, 6495.

(11) (a) Dybtsev, D. N.; Nuzhdin, A. L.; Chun, H.; Bryliakov, K. P.; Talsi, E. P.; Fedin, V. P.; Kim, K. *Angew. Chem., Int. Ed.* **2006**, *45*, 916. (b) Suh, K.; Yutkin, M. P.; Dybtsev, D. N.; Fedin, V. P.; Kim, K. *Chem. Commun.* **2012**, *48*, 513.

(12) Lin, L.; Yu, R.; Wu, X.-Y.; Yang, W.-B.; Zhang, J.; Guo, X.-G.; Lin, Z.-J.; Lu, C.-Z. *Inorg. Chem.* **2014**, *53*, 4794.

(13) Kuang, X.; Ma, Y.; Su, H.; Zhang, J.; Dong, Y.-B.; Tang, B. *Anal. Chem.* **2014**, *86*, 1277.

(14) Li, Z.-J.; Yao, J.; Tao, Q.; Jiang, L.; Lu, T.-B. *Inorg. Chem.* **2013**, *52*, 11694.

(15) Li, P.; He, Y.; Guang, J.; Weng, L.; Zhao, J.; Xiang, S.; Chen, B. *J. Am. Chem. Soc.* **2014**, *136*, 547.

(16) (a) Das, M.; Guo, Q.; He, Y.; Kim, J.; Zhao, C.-G.; Hong, K.; Xiang, S.; Zhang, Z.; Thomas, K.; Krishna, R.; Chen, B. *J. Am. Chem. Soc.* **2012**, *134*, 8703. (b) Yuan, G.; Zhu, C.; Xuan, W.; Cui, Y. *Chem. - Eur. J.* **2009**, *15*, 6428. (c) Li, G.; Yu, W.; Cui, Y. *J. Am. Chem. Soc.* **2008**, *130*, 4582.

(17) (a) Sang, R.-L.; Xu, L. *Chem. Commun.* **2013**, *49*, 8344. (b) Jhu, Z.-R.; Yang, C.-I.; Lee, G.-H. *CrystEngComm* **2013**, *15*, 2456. (c) Liang, X.-Q.; Li, D.-P.; Li, C.-H.; Zhou, X.-H.; Li, Y.-Z.; Zuo, J.-L.; You, X.-Z. *Cryst. Growth Des.* **2010**, *10*, 2596.

(18) (a) Li, J.-R.; Sculley, J.; Zhou, H.-C. *Chem. Rev.* **2012**, *112*, 869. (b) Cook, T. R.; Zheng, Y.-R.; Stang, P. J. *Chem. Rev.* **2013**, *113*, 734.

(19) (a) Xuan, W.; Zhang, M.; Liu, Y.; Chen, Z.; Cui, Y. *J. Am. Chem. Soc.* **2012**, *134*, 6904. (b) Wang, W.; Dong, X.; Nan, J.; Jin, W.; Hu, Z.; Chen, Y.; Jiang, J. *Chem. Commun.* **2012**, *48*, 7022. (c) Zhang, M.; Pu, Z.-J.; Chen, X.-L.; Gong, X.-L.; Zhu, A.-X.; Yuan, L.-M. *Chem. Commun.* **2013**, *49*, 5201. (d) Xie, S.-M.; Zhang, Z.-J.; Wang, Z.-Y.; Yuan, L.-M. *J. Am. Chem. Soc.* **2011**, *133*, 11892. (e) Tanaka, K.; Muraoka, T.; Hirayama, D.; Ohnish, A. *Chem. Commun.* **2012**, *48*, 8577.

(20) Jiang, J.; Babarao, R.; Hu, Z. *Chem. Soc. Rev.* **2011**, *40*, 3599.

(21) *APEX2*; Bruker AXS: Madison, WI, 2010.

(22) *SAINT Data Reduction Software*; Bruker AXS: Madison, WI, 2009.

(23) Sheldrick, G. M. *SADABS*; University of Göttingen: Göttingen, Germany, 2008.

(24) Farrugia, L. J. *J. Appl. Crystallogr.* **1999**, *32*, 837.

(25) Sheldrick, G. M. *SHELXL-97: Program for the Refinement of Crystal Structures*; University of Göttingen: Göttingen, Germany, 1997.

(26) Sheldrick, G. M. *Acta Crystallogr., Sect. A: Found. Crystallogr.* **1990**, *46*, 467.

(27) Sheldrick, G. M. *Acta Crystallogr., Sect. A: Found. Crystallogr.* **2008**, *64*, 112.

(28) (a) Wirth, T.; Kulicke, K. J.; Fragale, G. *J. Org. Chem.* **1996**, *61*, 2686. (b) Bagutski, V.; Elford, T. G.; Aggarwal, V. K. *Angew. Chem., Int. Ed.* **2011**, *50*, 1080. (c) Chubb, N. A. L.; Cox, M. R.; Dauvergne, J. S.; Ewin, R. A.; Lauret, C. U.S. Pat. Appl. Publ., 20070167506.

(29) Chen, L.; Reiss, P. S.; Chong, S. Y.; Holden, D.; Jelfs, K. E.; Hasell, T.; Little, M. A.; Kewley, A.; Briggs, M. E.; Stephenson, A.; Thomas, K. M.; Armstrong, J. A.; Bell, J.; Busto, J.; Noel, R.; Liu, J.; Strachan, D. M.; Thallapally, P. K.; Cooper, A. I. *Nat. Mater.* **2014**, *13*, 954.

(30) Dubbeldam, D.; Calero, S.; Vlugt, T. J. H. *Mol. Simul.* **2014**, *40*, 585.

DOI: 10.1021/jacs.5b06760
J. Am. Chem. Soc. 2015, 137, 12045−12049